Pergamon

PII: S0969-8043(96)00287-4

Appl. Radiat. Isot. Vol. 48, No. 6, pp. 815–831, 1997

Printed in Great Britain
0969-8043/97 $17.00 + 0.00

Systematic Effects of Total Cocktail Mass (Volume) and H_2O Fraction on $4\pi\beta$ Liquid Scintillation Spectrometry of ^3H

R. COLLÉ

Physics Laboratory, National Institute of Standards and Technology, Gaithersburg, MD 20899, U.S.A.

(Received 30 May 1996)

Detection efficiencies ϵ of ^3H by $4\pi\beta$ liquid scintillation (LS) spectrometry systematically vary as a function of both total cocktail mass m and cocktail composition (such as the H_2O mass fraction f). Quench indicating parameter (QIP) determinations, such as for the Horrocks number H, are also dependent on m and f. These systematic effects were investigated with a matrix of 33 LS cocktails covering a broad array of m and f values: 3.0 g $\leq m \leq$ 21.4 g and $0.002 \leq f \leq 0.52$. The effects of m and f on the LS background counting rates of matched blanks are also treated in detail. The uncertainties associated with these m- and f-dependent effects on ϵ and on H are particularly given close scrutiny. The systematics clearly demonstrate that efficiency changes cannot be adequately monitored by quench indicating parameters when the quench changes are induced by multiple causal factors (e.g. simultaneously varying cocktail sizes and compositions). The experimental results presented here have significant implications on the critical importance of understanding the systematics of these variable effects for a given LS system (combination of cocktails and spectrometer), and of *very closely* matching LS cocktail volumes and compositions in order to achieve reproducible and accurate LS counting results. © 1997 Published by Elsevier Science Ltd

Introduction

Zimmerman and Collé (1997) recently reported on an apparent energy-dependent effect of cocktail volume on detection efficiencies and quench indicating parameter (QIP) determinations in $4\pi\beta$ liquid scintillation (LS) spectrometry. They observed substantial systematic dependencies in both the efficiencies and determinations of QIP as a function of the total LS cocktail volume. The primary focus of their study, however, was to investigate the magnitude of possible volume effects on the assay of low-energy β-emitting radionuclides as obtained with a ^3H-standard efficiency tracing method (see, for example, their paper Zimmerman and Collé, 1997; as well as Collé and Zimmerman, 1996a, 1996b and references therein, for details on the invoked method). They evaluated the efficiency tracing method for assays of ^{63}Ni and ^{36}Cl traced against a ^3H standard for a sole cocktail composition (about 5% H_2O) over a cocktail volume range of nominally 5–20 mL. Despite rather large changes in LS detection efficiency and in the determination of QIP with volume, they found that the efficiency tracing could adequately correct for these effects *provided that the LS cocktails were closely matched in volume and composition*. With matched cocktails, the method excellently traced the massic activity of both ^{63}Ni and ^{36}Cl, almost invariantly of a given cocktail volume, to within the approximate $\pm$ 0.6% relative standard uncertainties for the LS measurement precision. The only exceptions were at the extremes of very small and very large cocktail volumes, particularly for the lower β-energy emitter ^{63}Ni. Zimmerman and Collé (1997) did not, however, explicitly address the uncertainty (actually an error in the true sense) introduced by a cocktail volume *mismatch* between the ^3H standard and traced radionuclide. Rather, they examined the possible effect (and associated uncertainty) of volume changes on the invoked ^3H-standard efficiency tracing method *when employing composition- and volume-matched cocktails*.

The LS detection efficiency of ^3H and QIP data presented in this paper are believed to be a useful adjunct to the work of Zimmerman and Collé (1997) in helping to understand the systematics of cocktail volume effects in $4\pi\beta$ LS spectrometry. The data presented here cover a slightly broader cocktail volume range (2.7–20.5 mL) and, more importantly, include five different H_2O fraction cocktail compositions ranging from less than 0.2% to over 50% H_2O. These compositions encompass both transparent homogeneous solutions and translucent counting

gels. Moreover, the primary intent of the present work was to investigate cocktail volume and composition *mismatch* effects.

The results of this study have significant implications which are addressed in a companion paper (Collé, 1997). The subsequent analyses (with examples) particularly focus on how cocktail mismatches (between LS counting sources) affect both comparative ^{3}H measurements (with or without quench curve corrections) and ^{3}H-standard efficiency tracing for other β-emitting radionuclides.

Contemporary readers may be surprised by the 'age' of the LS data presented herein. The experimental work was performed over 6 years ago at this laboratory for ancillary experiments that were used for a much larger investigation of the ^{3}H-standard efficiency tracing of ^{214}Pb and ^{214}Bi in ^{222}Rn subseries decay (Collé, 1995). These ^{3}H data have not been previously presented or published, and were largely 'buried' within various small corrections applied to the determination of the LS detection efficiency for ^{222}Rn. The wealth of data (and its significance) was only recently 'rediscovered.' These original (somewhat-aged) data were, as a result, completely re-analyzed and interpreted in an entirely new light for the purposes of the present study.

Experimental Aspects

Overview of the cocktail preparations and compositions

Thirty-three ^{3}H counting sources of varying total cocktail mass and varying aqueous mass fraction were prepared by gravimetric additions of three components: a commercial scintillation fluid with mass m_c; blank water (to vary the H_2O fraction) with mass m_w; and a sample of tritiated water with known ^{3}H activity concentration and mass m_s. An additional 33 matched blanks (for background counting subtractions) with nearly identical composition, but without m_s, were also prepared.

The cocktail components were sequentially introduced into nominal 20 mL, borosilicate glass, flame-sealable LS vials. After filling, the vials were subsequently flame sealed using a 'natural gas' (methane)/oxygen torch. While sealing the vials, the volatile (and flammable!) cocktail was frozen with an especially-designed cryostat that maintained a temperature of about 200 K (-77 to -72°C) as obtained with a solid CO_2 ('dry ice')/isopropanol slurry (Collé, 1995).

The prepared ^{3}H cocktails (and 33 matched blanks) formed a matrix of compositions with varying total cocktail mass $m = m_c + m_w + m_s$ and H_2O mass fraction $f = (m_w + m_s)/m$. The relative standard uncertainty in any determination of m or f is estimated to be about $\pm 0.1\%$. Assuming a scintillation fluid density of $\rho \simeq 0.92$ g mL^{-1} (as determined by this laboratory) and a H_2O density of unity, the total cocktail volume V (in mL) for any of the compositions can be approximated by $V \simeq m - m_c(1 - 1/\rho) = m[1 - (1 - f)(1 - 1/\rho)] \simeq m(1.087 - 0.087f)$.

The matrix of cocktails is illustrated in Fig. 1. As indicated, the matrix slices across seven m values and across five f values. The cocktails in the lower two f slices ($f \simeq 0.002$–0.016 for the lowest, and about $f \simeq 0.14$ for the next) are transparent solutions, and the upper three (about $f \simeq 0.27$, 0.34 and 0.52) are gels. The former two solution cocktails nicely complement the single composition data given by Zimmerman and Collé (1997) for an aqueous fraction of about $f \simeq 0.05$.

Gravimetric determinations of the cocktail components

Mass determinations for m_c and m_w were performed with a single-pan suspension balance having calibrated internal balance reference weights and 0.1 mg scale sensitivity. Any single determination of the mass for these m_c and m_w components is estimated to have a relative standard uncertainty of less than about $\pm 0.05\%$ for a mass $m > 1$ g to about $\pm 0.1\%$ for 0.1 g $< m <$ 1 g.

Masses of m_s were obtained with a more sensitive (1 μg) single-pan suspension microbalance which also employed calibrated internal balance reference weights. These determinations of m_s have an estimated uncertainty, corresponding to an assumed standard deviation, of $\pm$ 10–30 μg. For samples of about 50 mg, the relative standard uncertainties in the sample mass measurements are thus about $\pm$ 0.02–0.06% after appropriate gravimetric measurement air-buoyancy corrections, and considering the internal-balance-weight corrections and uncertainties, and typical mass measurement precision. Typical air-buoyancy corrections, on a relative

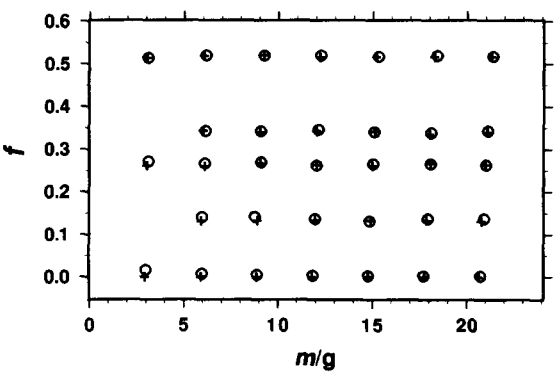

Fig. 1. Matrix of 33 LS cocktail compositions used in this study. The abscissa m (in g) is the total cocktail mass contained in a 20 mL LS counting vial. The ordinate f is the mass fraction of H_2O in the cocktail. Cocktails containing ^{3}H are represented by the open circles (○) while the matched blanks are shown as crosses (+).

basis, are about + 0.1% for solutions with densities of near unity (i.e. 0.8–1.1 g mL^{-1}). Internal balance weight corrections (obtained from double-substitution weighings with calibrated references masses and sensitivity weights of 1–10 mg) are typically less than ± 10 μg (for any combination of balance weights < 1 g).

The aliquant mass m_s for every cocktail was also verified from two independent mass determinations: a pycnometer-dispensed mass difference (called a 'dispensed mass') and a 'contained mass' obtained from the difference between the final mass and initial tare mass of the containing vessel. Differences between the 'dispensed mass' and 'contained mass' (which rely on wholly different internal balance weights for the various four mass readings) were typically less than 0.01–0.02% for sample masses of about 50 mg.

Cocktail components

The employed scintillator fluid was 'PCS', a xylene-surfactant-based scintillator (Amersham Corp., 1981) which is capable of handling aqueous samples over a very broad range of H_2O fractions. Below about 15% H_2O, aqueous samples in PCS form transparent, homogeneous counting solutions. Above about 22% H_2O (up to nearly 70% water as observed by this laboratory), the mixes form a countable translucent gel. Between these H_2O fractions, the mixes form an immiscible, two-phase, non-countable region. This admirable scintillator, regrettably, is no longer commercially available, having been supplanted by 'environmentally safe' (i.e. non-toxic, non-flammable, and bio-degradable) fluids such as the equally high-water-loading 'Instagel'. Yet, in just the past year (December 1995), a 6-year-old cache of PCS (said to be from its last production run and which had been secured and stored by our laboratory) was still found to be stable and viable. Furthermore, various limited comparisons by our laboratory between PCS and currently available 'environmentally safe' fluids, such as 'Ready Safe', 'Ultima Gold', and 'Instagel' largely confirm (but with substantially less data) the systematic volume and cocktail composition trends that will be presented here. Masses of PCS in the various volume-varying cocktails ranged from $m_c \simeq 1.5$ to 20.6 g.

Blank H_2O, which was used to vary the aqueous mass fraction of the cocktails and to prepare matched counting blanks of nearly identical cocktail composition for every ^3H counting sample, consisted of aged, ion-exchanged, doubly-distilled, 'tritium and radon free' water having a total α- or β-emitting radionuclidic impurity, in terms of an equivalent ^3H massic activity, of less than (0.008 ± 0.004) Bq g^{-1}. Added quantities of the blank H_2O varied from $m_w = 0$ (for samples with minimum aqueous mass fraction) up to $m_w \sim 11$ g.

The tritiated water aliquants for the LS cocktails were obtained from a standard ^3H solution which in turn was obtained from a careful gravimetric dilution of SRM 4927D (National Institute of Standards and Technology, 1989) with a dilution factor of $D = 21.02 \pm 0.01$. The dilution was performed with the same H_2O used to prepare the matched counting blanks. SRM 4927D was certified to have a ^3H massic activity of $(6.286 \pm 0.052) \times 10^5$ Bq g^{-1} as of 1200 EST 1 January 1989, where the cited uncertainty is assumed to correspond to a three standard deviation interval. Approximately $m_s \simeq 42$–50 mg of the diluted ^3H standard solution (in which, as noted, each aliquant was determined to a relative uncertainty of better than ± 0.05%) was added to each of the 33 cocktails.

LS spectrometer characteristics

The spectrometer used for the measurements was a Beckman LS7800 model LS counter which was equipped (on modification) with: (i) two Hamamasutu R331-05 photomultiplier tubes (PMT) operating in a coincidence mode; (ii) a logarithmic amplifier (for the summed coincident pulses) coupled to an analog-to-digital converter (ADC) for spectral pulse-height analyses; (iii) circuitry for the determination of counting live times (to within about ± 0.1%) by counting timing signals from a gated oscillator; and (iv) an external ^{137}Cs source for Compton-edge quench monitoring. The resolving time of the coincidence gate for simultaneous detection of singles PMT events was 22 ns. The instruments's resolving time for conversion of the summed coincident pulses was dependent on pulse height and varied from 5 to 33 μs.

The QIP employed by the spectrometer is an internally-derived Horrocks number (H) which is based on the downward spectrum shift of the Compton edge of the external ^{137}Cs γ-ray source with increasing quenching in the LS cocktail. The parameter H corresponds to the spectral channel number shift between the quenched cocktail and an unquenched blank reference cocktail. The channel number shift $H = (c_1 - c_2)$ is, because of the logarithmic pulse amplification, proportional to the logarithmic energy ratio $H \sim \log(E_2/E_1)$.

Counting conditions and calculations

During the period 29 July–6 August 1989, the entire series of ^3H cocktails and blanks (interspersed alternately) were replicately measured five times, each for 3000 s. The counting rate on any given sample ranged from about 270 s^{-1} (for the cocktail, as expected, with minimum mass of $m \simeq 3$ g and maximum $f \simeq 0.5$ with a ^3H efficiency of about $\epsilon \simeq 0.18$) to about 640 s^{-1} (for the cocktail with apparently optimal mass $m \simeq 9$ g and minimum $f \simeq 0.005$ with a ^3H efficiency of about $\epsilon \simeq 0.48$). Background counting rates on the matched blank cocktails for any given measurement cycle ranged from about 0.6 s^{-1} (at minimum m and

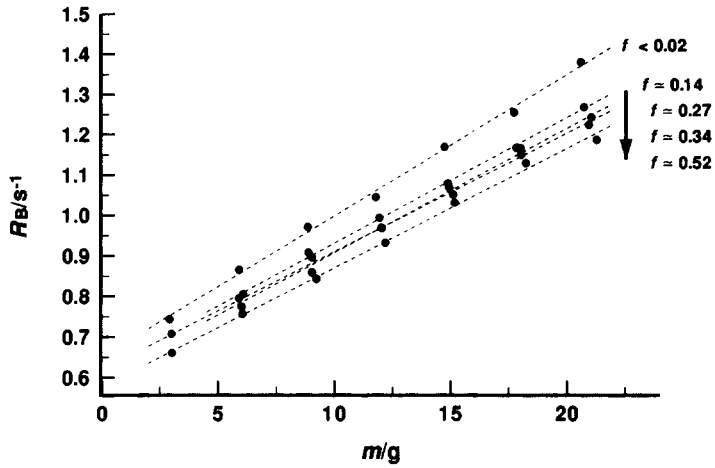

Fig. 2. LS background counting rates R_B (in s^{-1}) as a function of the total cocktail mass m (in g) for five cocktail compositions having a H_2O mass fraction f. The dashed lines are fits of the data (for a given constant f) to a linear function $R_B = a + b \cdot m$ with the slope b in the range $dR_B/dm \simeq 0.03\ s^{-1}g^{-1}$ for any $0.14 \leq f \leq 0.52$ and $dR_B/dm \simeq 0.035\ s^{-1}g^{-1}$ for $f < 0.02$.

thereby having least geometrical detection efficiency and for the largest f with maximal quenching by the imposed H_2O) to 1.4 s^{-1} (at maximal m and minimal f).

The LS detection efficiency $\epsilon_{j,i}$ for a given ^3H cocktail j from measurement cycle i at time $t_{j,i}$ was determined from the relation: $\epsilon_{j,i} = [R_{T(j,i)} - R_{B(j,i)}]/[m_{s(j)} \cdot (C_T/D) \cdot \exp(-\lambda t_{j,i})]$ where $R_{T(j,i)}$ is the uncorrected count rate for ^3H sample j in measurement cycle i; $R_{B(j,i)}$ is the count rate of the corresponding matched blank cocktail j obtained during measurement cycle i; $m_{s(j)}$ is the mass of the aliquant of the calibrated ^3H solution used; C_T is the certified ^3H massic activity of SRM 4927D at its reference time t_0 (given previously); D is the gravimetrically determined dilution factor for relating C_T to the ^3H massic activity of the diluted and calibrated solution (also given previously); and $\exp(-\lambda t_{j,i})$ is a ^3H decay correction for the assumed ^3H decay constant $\lambda = (\ln 2)/(12.43 \pm 0.05a)$ (National Institute of Standards and Technology, 1989) and for the time interval $t_{j,i}$ between t_0 and the midpoint time for measurement of sample j during cycle i.

The ^3H detection efficiency for any given cocktail composition was obtained by averaging the individual $\epsilon_{j,i}$ values over the five measurement cycles to obtain a mean ϵ_j for the given total cocktail mass m_j and aqueous mass fraction f_j. Similarly, the five individually determined QIP values for each cocktail $H_{j,i}$ were averaged to obtain a mean H_j for the jth cocktail. Uncertainty estimators for the replicate measurement precision of both the mean ϵ_j and mean H_j were taken to be their respective standard deviations of the mean (s_m) for $\nu = 4$ degrees of freedom.

Measurement Results and Discussions

Effects of m *and* f *on counting backgrounds*

The results of the background counting rates R_B of the 33 matched blanks clearly demonstrate two somewhat predictable effects of m and f. These results are shown in Fig. 2. As indicated, R_B, in all cases, increases nearly linearly with increases in m. This direct proportionality of R_B to m is just a manifestation of the increased sensitivity (as m increases) of a larger and larger scintillation detector to external radiations (e.g. environmental γ rays and cosmic rays). Secondly, the data of Fig. 2 clearly demonstrate the effect of quenching on the LS detection efficiency for even external radiations. Again, in all cases, R_B (for constant m) increases (indicating increasing detection efficiency) with decreasing f (and decreasing quenching by the imposed H_2O). Hence, the smallest backgrounds are obtained with minimum m (smallest geometrical detection efficiency) or maximum f (largest quenching); while the largest backgrounds are obtained under the converse conditions of maximum m or minimum f. In the region between these two extremes, the magnitudes of the effects of m and f on R_B are such that neither variable completely dominates. For example, the observed R_B at $m \simeq 9$ g with low quenching ($f \simeq 0$) is greater than that at $m \simeq 12$ g with large quenching ($f \simeq 0.5$). These competing effects can have important implications for very low-level measurement applications where one must balance the advantage of larger sample aliquants in large cocktail volumes (to increase net count rates) against the disadvantages of correspondingly larger backgrounds and/or greater quenching. *C'est à dire*, Collé and Thomas (1993), to verify one step in the serial dilutions used in the preparation of $^{36}Cl/Cl$ accelerator-mass-spectrometry standards, had to optimize between the need for large cocktail volumes and sample sizes (multiple-gram aliquants in relatively large scintillator volumes in order to measure a 0.035 Bq g^{-1} ^{36}Cl solution whose net LS count rate was only a few percent of background) and the contrary need for small cocktail volumes (in order

to minimize the geometrical detection efficiency for the background and aliquant-size-dependent quenching effects).

Background-determination uncertainty and elucidation of its components

The uncertainties in the determination of R_B (see Table 1), in terms of a relative standard deviation of the mean (coefficient of variation) for 5 replicate measurements of each blank, ranged from about $v_m(R_B) = 100 \cdot s_m(R_B)/R_B \simeq 1.4\%$ to $v_m(R_B) \simeq 4.2\%$, and were independent of m and f, as well as of the magnitude of R_B. These invariances of m and f on R_B [and magnitudes of $v_m(R_B)$] indicate that the background reproducibility is not dominantly controlled by the statistical Poisson 'counting errors' for R_B, but rather must have substantial contributions from either the inherent precision for the LS measurement process or the variability in the ambient background radiation itself. [As an aside: one must bear in mind in examining Table 1 that the wide dispersion of $v_m(R_B)$ values arises from the broad χ^2 distribution of $s_m(R_B)$ values for 4 degrees of freedom, that is in turn associated with the random sampling of R_B values from even an assumed normal distribution.]

One can go one step further and establish some crude estimates on the magnitudes of the uncertainty components comprising $v_m(R_B)$. With assumptions as to the underlying error model, the relative uncertainty on any one determination of R_B for any cocktail (as obtained from the five replicate measurements) can be expressed as $v_m(R_B) \simeq [v_C^2 + v_{LS}^2 + v_B^2]^{1/2}$ where v_C is the overall Poisson 'counting error', v_{LS} is a measure of the inherent LS measurement precision (repeatability) over the five measurements, and v_B is an estimator for the uncertainty due to the actual ambient background variability. The product of background counting rates of about 0.6–1.4 s^{-1} and the 3000 s counting time intervals and the five measurements, yields a total count number of about 9000–21000, from which one may approximate the relative 'counting error' to be about $v_C \simeq 1.1$–0.7%. The median is $v_C \simeq 0.9\%$. From Section 3.6 below, v_{LS} may be derived by considering the observed estimates of the relative standard deviation of the mean for the replicate measurements of the ^3H detection efficiencies (in which the Poisson 'counting errors' are fairly negligible). These 33 estimates of v_{LS} over all cocktail compositions range from about 0.08 to 0.76% (in a worst case) with an overall mean value of 0.21%. The more robust median value (0.18%) is wholly compatible. From the 33 data given in Table 1, the mean and median values of $v_m(R_B)$ are $\simeq 2.3$ and $\simeq 2.5\%$, respectively. Hence, with estimates of $v_m(R_B) \simeq 2.4\%$, $v_C \simeq 0.9\%$, and $v_{LS} \simeq 0.2\%$, the uncertainty for the inherent ambient background variability may be taken to be $v_B \simeq [v_m(R_B)^2 - v_C^2 - v_{LS}^2]^{1/2} \simeq 2.2\%$. So, in this particular case, it is apparent that the v_B component nearly dominates the $v_m(R_B)$ uncertainty, and appears to be at least double v_C. This, however, is not necessarily always the situation. Data from other LS experiments conducted by this laboratory over the past decade or so have exhibited other cases. One can, of course, always make v_C be the dominant component by merely failing to accumulate a sufficient total number of background counts. However, even when v_C is made negligible with respect to $v_m(R_B)$ (by counting for very long time intervals), situations have been encountered where the measurement precision reflected in v_{LS} was substantially greater than the ambient background variability component v_B. Largely, these situations can be attributed either to measurement system instabilities (e.g. peculiar spectrometer malfunctions or irregularities due to less stable cocktail compositions) or to time periods of unusually stable, incident background radiation fluxes. In fact, our laboratory has generally found that $v_{LS} > v_B$, particularly when v_{LS} is estimated from measurements with low-energy β-emitters.

Astute readers will easily deduce how they may apply similar analyses to their LS counting background data to understand the underlying background components. Appreciation of the relative magnitudes of v_{LS} and v_B for their LS measurement systems (at any given time) can be a benefit to quality assurance monitoring of their laboratory practices and their spectrometers' performance.

Table 1. Variability in LS background counting rates R_B, in terms of the relative standard deviation of the mean (coefficient of variation) $v_m(R_B)$ obtained from five replicate measurements, for 33 cocktail compositions having a total mass m and H_2O mass fraction f

	$v_m(R_B)$ (in %)				
Range of m (in g)	$f < 0.02$	$f \simeq 0.14$	$f \simeq 0.27$	$f \simeq 0.34$	$f \simeq 0.52$
2.9–3.0	2.8	—	2.5	—	3.3
5.9–6.1	2.8	4.2	3.0	1.4	1.9
8.8–9.2	2.1	2.5	3.1	2.2	1.7
11.8–12.2	2.5	2.8	2.2	2.5	2.6
14.7–15.2	1.9	1.4	3.8	3.5	1.5
17.8–18.2	2.1	2.0	2.2	3.3	1.4
20.6–21.3	2.6	2.0	2.3	1.2	2.0

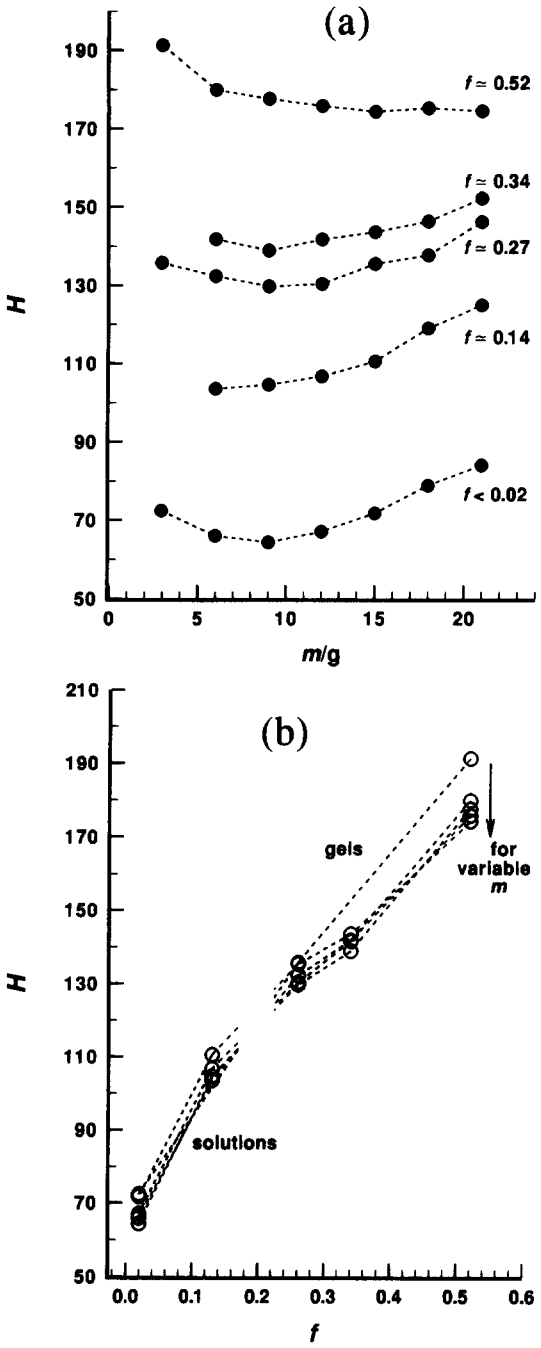

Fig. 3. Variation of the Horrocks number H quench indicating parameter: (a) as a function of total LS cocktail mass m (in g) for five cocktail compositions having a H_2O mass fraction f; and (b) as a function of f for seven series of LS cocktails with total mass m.

Effects of m *and* f *on the QIP Horrocks number*

Figure 3(a,b) displays the systematics of the QIP Horrocks number H as a function of m and f. As indicated, H is considerably more sensitive to changes in f (over the range $0.002 \leq f \leq 0.52$) than to any changes in m (over its $2.9\ \text{g} \leq m \leq 21\ \text{g}$ range): H vs m (for constant f) varies by less than 10–30% for any of the five cocktail compositions [Fig. 3(a)]; whereas H (for any given constant m) changes by well over a factor of 2 across the range of f values [Fig. 3(b)]. In fact, if one views Fig. 3(b) with a slightly jaundiced eye it might be imagined (on gross appearance) that H vs f is almost given by a single functional (nominally linear) relationship that is nearly independent of m. This gross effect can be understood if one considers an idealized quenching situation.

Quenching is a collective term, and is normally defined to be any effect or imposed agent that results in a diminished LS detection efficiency (i.e. anything that obstructs the conversion of a radionuclide's decay energy into light photons that are emitted from the LS cocktail and detected by the spectrometer's PMT). This can consist of, for example, (i) 'chemical quenching' in which there is an incomplete transfer of energy from say a ^{3}H β-particle to the scintillation fluor because of energy loss collisions with other molecules in the cocktail (e.g. with the many kinds in the complex mix of the scintillation fluid itself which is composed of solvents, surfactants, chemical waveshifters, emulsifiers, etc.; as well as with any imposed sample molecules such as water, acids, dissolved salts, etc.) or (ii) 'optical quenching' (sometimes called 'color quenching') in which the light photons emitted by the fluor get absorbed by the components of the cocktail (or even by the vial walls, impurities on the walls, etc.) before reaching the PMT, or get shifted to photo-energies that are insufficient to produce photoelectrons in the PMT). In the ideal then, the *internal* quenching (whether chemical or optical) in a cocktail, which is quantified by some QIP, would only be influenced by the composition of the cocktail and not by any extraneous external influences. Hence, this idealized QIP should only vary predictably with any regular or systematic changes in the cocktail composition. A linear QIP, for example, would be expected to vary linearly with any linear measure of a cocktail composition variable. For the relatively simple ^{3}H cocktails (pure H_2O in PCS) used here, having a linear H_2O mass fraction f composition parameter, one might indeed expect a linear QIP would just be directly proportional to f.

The H determinations given here obviously do not adhere to this ideal since they are affected by m (even with constant f). It can be argued that the apparent dependence of m on H must consist of both an internal quenching and some external effect. If it were a pure internal quenching effect, one would expect to observe an unrestrictive monotonic increase in H (and in quenching) with increasing m because of the corresponding increases in the average path length $x_{h\nu}$ for the fluorescent photons which would result in greater $\exp(-\mu x_{h\nu})$ absorption losses (where μ is some overall light absorption coefficient). Of necessity, $x_{h\nu}$ is some increasing geometric function G of m; $x_{h\nu} \sim G(m)$. Internal quenching due to energy-loss collisions of the β-particles before they reach the fluor molecules is not, however, a factor.

The average path length x_β for the β-particles between the decaying ^3H radionuclides and fluor molecules is independent of m changes inasmuch as the cocktails may be assumed to consist of a homogeneous mix of the ^3H_2O and fluor molecules. Hence, the energy losses dE_β/dx_β would be very similar for cocktails of any m (with constant f). The abrupt changes in slope for the H vs m data [Fig. 3(b)] suggest that there must be some other external influence. The most likely causal factor may be the geometrical arrangement among the quench monitoring γ-ray source, the LS cocktail vial, and the PMT locations (and their respective subtended solid angles which would be m dependent). The effective subtended solid angles of this geometrical arrangement is also affected by the sensitivity of the PMT to fluorescent photons as one moves across the face of the PMT (the center generally being most sensitive, with increasingly less sensitivity as one moves toward the perimeter of the PMT face).

These variations in H as a function of m for the five f compositions exhibit a very curious feature. With increasing f (and increasing quenching), the dependence of H on m tends to flatten; i.e. the change in H with mass dH/dm is much less at large f (or H) values than at small ones. This is more evidently demonstrated with the renormalized data in Fig. 4. In regard to the magnitude of the variations for H in Fig. 4, it may be of interest to note that the changes in H for the lowest f composition ($0.002 \leq f \leq 0.02$) are very close to that found by Zimmerman and Collé (1997) for a composition of $f \simeq 0.05$ with ^3H solutions in another scintillation fluid ('Ultima Gold'). Their recent data for $f \simeq 0.05$ over a comparable m range nicely fall between that given here for the $0.002 \leq f \leq 0.02$ and $f \simeq 0.14$ compositions and follow the same general trends.

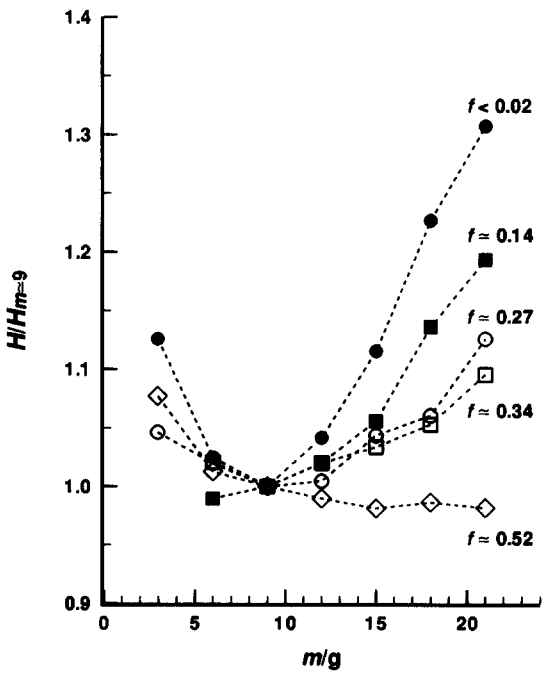

Fig. 4. Relative variations in normalized Horrocks number H quench indicating parameters [data of Fig. 3(a)] as a function of m for the five f cocktail compositions. The ordinate is the comparison ratio $H/H_{m\simeq 9}$ for H at any given m reduced by that for $m \simeq 9$ g.

In examining the gross features of Fig. 3(a,b) it is important to keep in mind that the displayed complex of data is highly convoluted in that two cocktail compositions are transparent solutions and three are translucent gels. One should not then place too much emphasis on any continuity of the functional relationship between H and f over the two counting regions.

Non-effects of m *and* f *on the uncertainty in Horrocks number QIP determinations*

The uncertainty associated with QIP determinations is an important consideration in implementing quench corrections, such as by use of simple quench curves or by more exacting efficiency-tracing methods. Therefore, how m and f might affect the precision (repeatability) in determining the QIP is also of considerable interest. This question is exhaustively examined in the six traces [labelled (a)–(f)] of Fig. 5. They consider the variability in H in terms of both a standard deviation of the mean $s_m(H)$ for the five replicate determinations of each H and its coefficient of variation $v_m(H) = 100 \cdot s_m(H)/H$. The two estimators $s_m(H)$ and $v_m(H)$ distinguish between uncertainties that may or may not be dependent on the magnitude of H (i.e. on the degree of quenching).

As seen in Fig. 5(a,b), both $v_m(H)$ and $s_m(H)$ seem to scatter randomly and are largely independent of m. More detailed examinations of the individual data values support this conclusion. Comparisons of determinations having very comparable H magnitudes (but very different m values) indicate that the precision is virtually invariant of m. Similarly, in Fig. 5(d), $s_m(H)$ appears to be independent of f. However, in contradistinction, $v_m(H)$ vs f [Fig. 5(c)] appears to be dependent on the magnitude of f. Since f and H are so highly correlated, one cannot distinguish if this $v_m(H)$ dependence is truly due to an effect of f or to H itself. Figure 5(e,f) can be used to support this argument. Again, it is clear that $s_m(H)$ generally scatters about $0.3H$ units invariantly of H [Fig. 5(f)]; whereas $v_m(H)$ decreases from around 0.5% at $H \simeq 60$ to about 0.2% at $H \simeq 180$. From all of the above, one reasonable interpretation is that the precision in determining QIP is largely independent of m and f and is also independent of the magnitude of H itself. In other words, the uncertainty in determining H is largely a fixed quantity and may be expressed by a given number of H units ΔH. Here (i.e. for the case of the present system of cocktails and spectrometer), $\Delta H = s_m(H) \simeq 0.3$ (for five replicate determinations). This in turn would seem to imply that the uncertainty in the determination of H is

merely a reflection of the precision (call it Δc) in being able to locate the position (channel number) of the inflection point of the Compton edge for the external γ-ray source that is used for quench monitoring, irrespective of the magnitude of the downward spectrum shift of the Compton edge with quenching. For H units, the uncertainty ΔH would then just be the uncertainty Δc.

One cannot help but wonder if the above finding is equally applicable to other external-source, non-Horrocks-number variants on Compton-spectrum-based quench monitoring. It may very well be

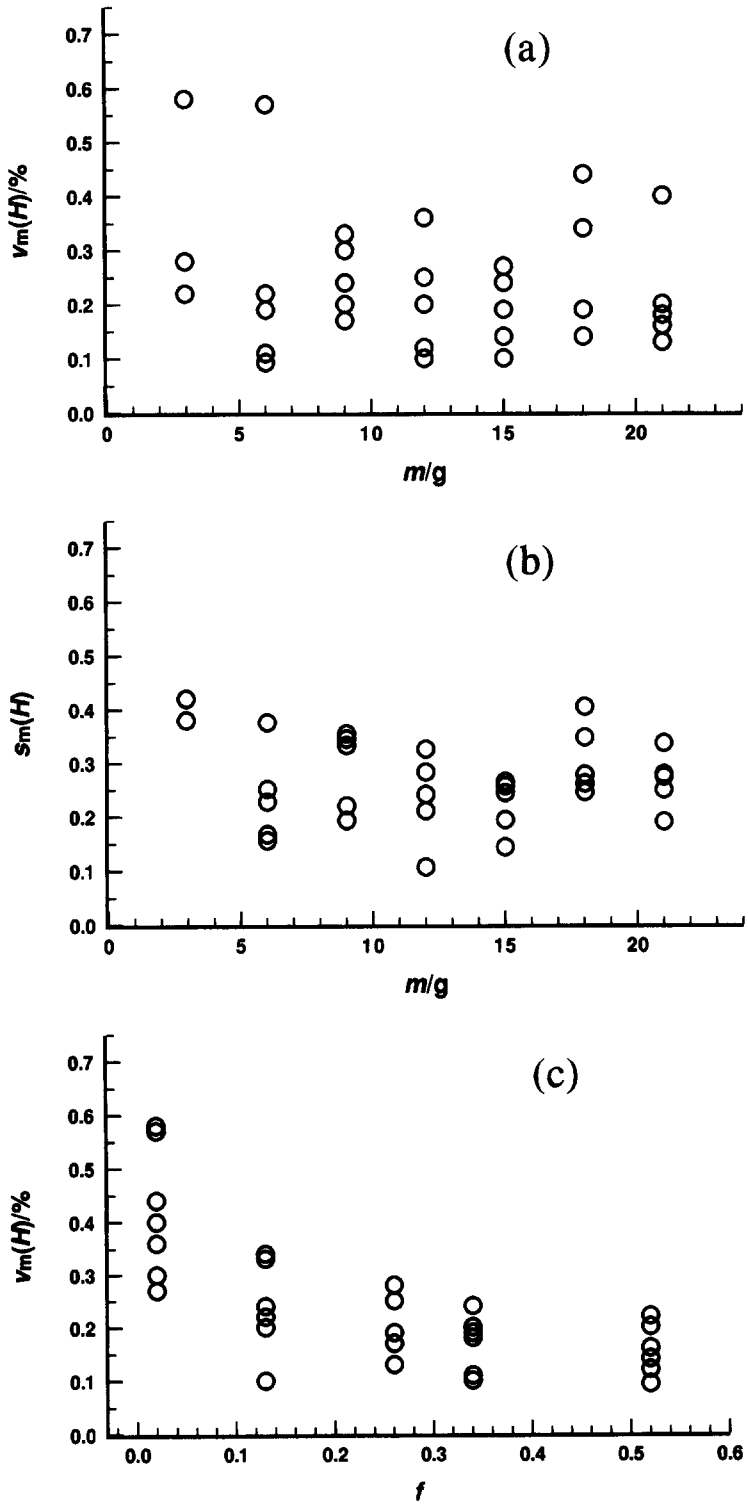

Fig. 5. (a–c). *Continued opposite.*

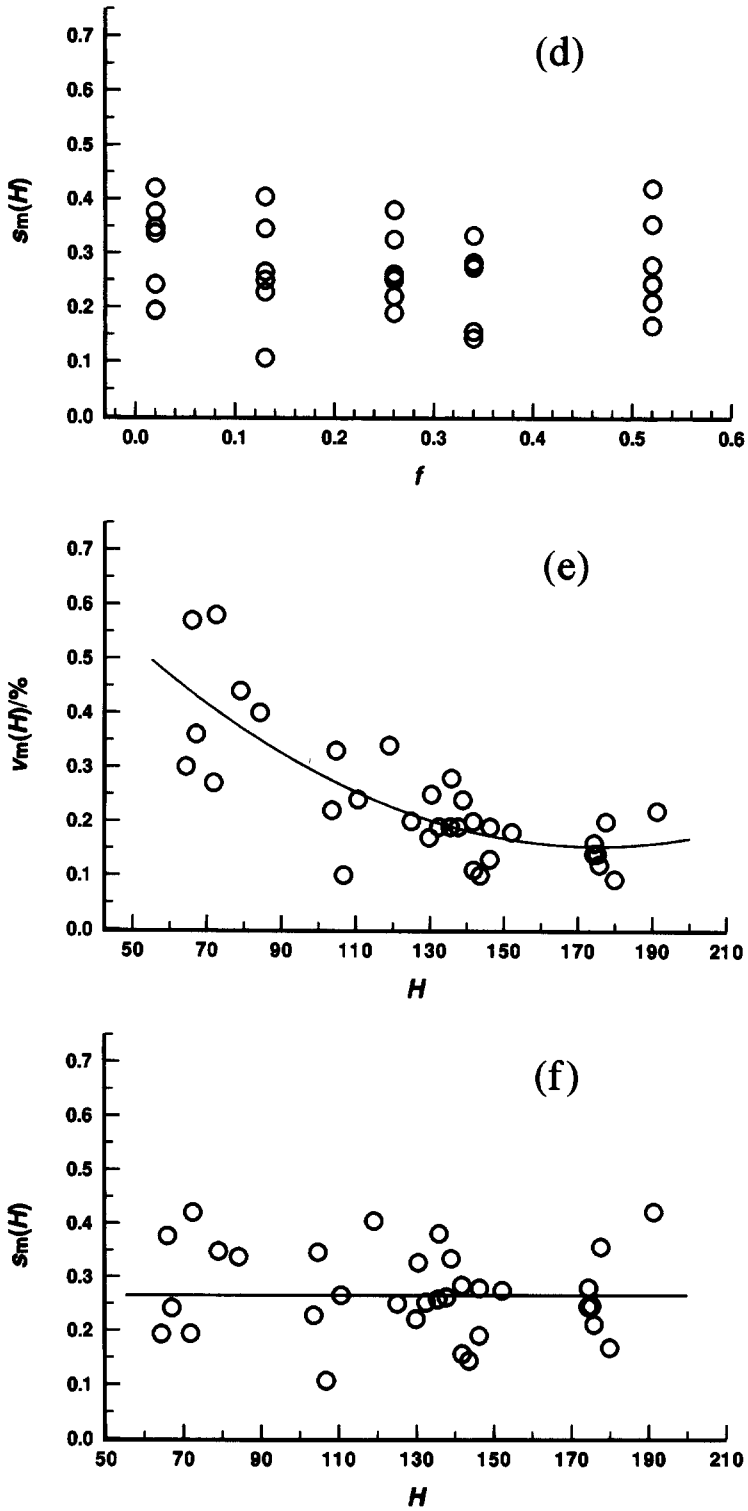

Fig. 5. Uncertainties for the determination of the Horrocks number H quench indicating parameter in terms of the standard deviation of the mean $s_m(H)$ (for five replicate determinations) and its corresponding coefficient of variation $v_m(H) = 100 \cdot s_m(H)/H$ (in %) as functions of total cocktail mass m [traces (a) and (b)], H_2O mass fraction f [traces (c) and (d)], and H [traces (e) and (f)]. The results demonstrate that the uncertainty in determining H is largely of fixed magnitude and independent of m, f and H.

applicable with some other types of Compton-spectrum-based QIPs since the explanation that the uncertainty in determining QIP is just a reflection of the uncertainty in locating the position (channel number) of some aspect of the Compton spectrum (be it the edge, or mean spectral energy, etc.) is a quite

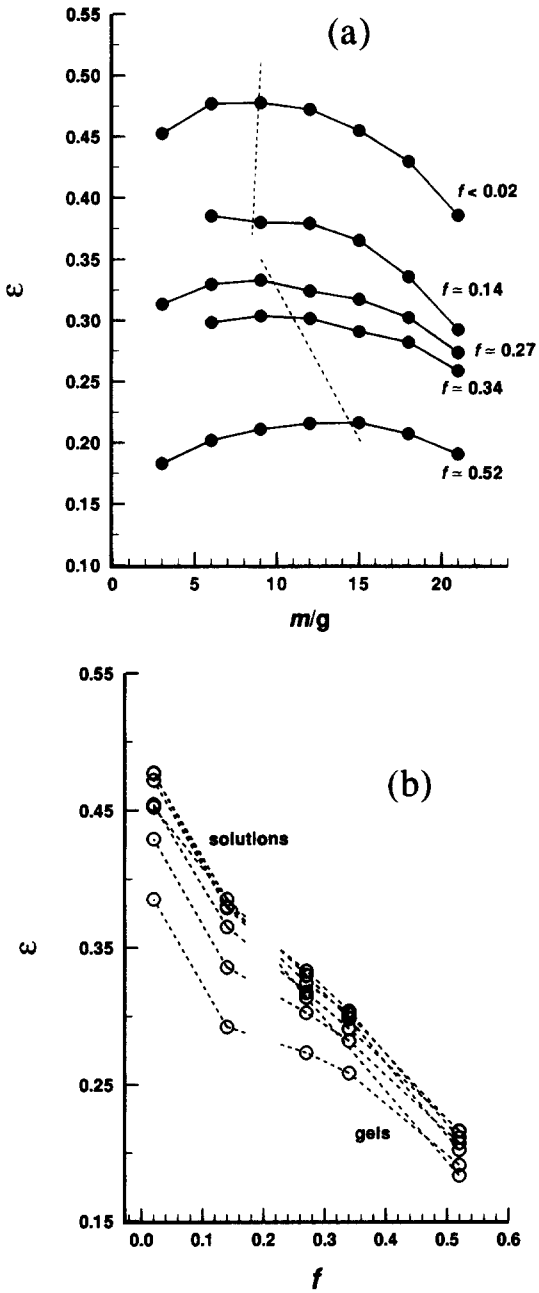

Fig. 6. Variation of the LS detection efficiency ϵ for ^{3}H: (a) as a function of the total cocktail mass m (in g) for five series of cocktail compositions having H_2O mass fraction f; and (b) as a function of the H_2O mass fraction f for seven series of cocktails with total mass m.

plausible expectation, provided that the Compton spectrum is not seriously degraded (flattened) on quenching and is in all cases defined with comparable counting statistics. An investigation of the nature of the uncertainty in QIP determinations for other external-source, Compton-spectrum-based quench monitoring methods is underway in this laboratory.

Effects of m *and* f *on detection efficiency for* ^3H

Figure 6(a,b) exhibits the systematics of the variations of the LS detection efficiency ϵ for ^{3}H as a function of m and f. The gross features are inversely related to that observed [Fig. 3(a,b)] for the dependencies of H on m and f. This is hardly surprising since H was designed and intended to mirror quench changes in ϵ. As H increases, ϵ decreases; and vice versa.

For the series of solution cocktails of lowest f (least quenched), the ^{3}H efficiencies vary from a maximum of around $\epsilon \simeq 0.48$ at $6\text{ g} \leq m \leq 9\text{ g}$ to about $\epsilon \simeq 0.38$ at $m \simeq 21$ g. The next solution series with $f \simeq 0.14$ parallels this: maximum $\epsilon \simeq 0.39$ at $6\text{ g} \leq m \leq 9\text{ g}$ and minimum $\epsilon \simeq 0.29$ at $m \simeq 21$ g. These trends again comport excellently with that observed by Zimmerman and Collé (1997) for solution cocktails with $f \simeq 0.05$ using a different scintillation fluid. They, in fact, concluded that the observed 'optimum' cocktail volume (in terms of maximum efficiency and minimum quenching) of 7–10 mL appeared to be somewhat lower than the canonically accepted value of 8–12 mL. This 'optimum volume' not only held for ^{3}H but also for ^{63}Ni and ^{36}Cl. The results given here for the solution cocktails support their concluded finding. However, this generalization is not true for the cocktail gels.

As seen in the three lower curves of Fig. 6(a), the maximum efficiency is shifted to larger m values as f increases. The maximums occur at $m \simeq 9$ g for $f \simeq 0.27$, $m \simeq 12$ g for $f \simeq 0.34$, and $m \simeq 15$ g for $f \simeq 0.52$. The appearance of a corollary effect in the QIP data [Figs 3(a) and 4] is not as pronounced, but exists.

The section above noted the lessening of the H dependence on m with increasing f. This is equally manifest in the efficiency data as redundantly demonstrated by the general flattening of the ϵ vs m curves [Fig. 6(a)] as f increases, and in the wider spread of ϵ for the various m values [Fig. 6(b)] at small f compared to that at large f.

A quite important consideration is whether the observed efficiency ϵ dependencies on m and f actually track (in an inverse fashion) the correlated changes in the quench parameter H with m and f. One convenient way to examine this is to consider the quantities $C_f = -(\partial H/\partial f|_m)/(\partial \epsilon/\partial f|_m)$ and $C_m = -(\partial H/\partial m|_f)/(\partial \epsilon/\partial m|_f)$ which should remain fairly constant if any change in ϵ by m or f is almost exactly matched by a corresponding change in H. These quantities may be approximated by $(H_1 - H_2)/(\epsilon_1 - \epsilon_2)$ for pairwise (adjacent) comparisons of the changes in H and ϵ with $\partial f|_m$ and $\partial m|_f$, and are very sensitive for small changes in efficiency $(\epsilon_1 - \epsilon_2)$ which occur, for example, at the relatively flat portions of the ϵ vs m dependence [Fig. 6(a)]. The quantities C_f and C_m would be exactly constant for a pure linear relation between ϵ and H. They are undefined (asymptotically approaching infinity) when ϵ is nearly independent of H and of quenching (e.g. for very high-energy β emitters or α emitters).

Table 2 shows the relation between C_f and varying f for the seven m cocktail sizes. Collectively, excepting

Table 2. Tracking of the quench indicating parameter H with the LS detection efficiency ϵ for ^{3}H due to changes ∂f in cocktail H_2O mass fraction f at near constant cocktail mass m as given by the quantity C_f. The assigned uncertainties correspond to a standard deviation of the mean $s_m(C_f)$ for 4 degrees of freedom (i.e. for the five replicate measurements of each H and ϵ used to determine C_f. Values in parentheses represent those for ∂f changes that correspond to transitions from solution to gel cocktails

	$C_f = -(\partial H/\partial f\|_m)/(\partial\epsilon/\partial f\|_m)$			
Range of m (in g)	$\partial f > (0.02–0.14)$	$\partial f \simeq (0.14–0.27)$	$\partial f \simeq (0.27–0.34)$	$\partial f \simeq (0.34–0.52)$
2.9–3.0	(456 ± 6)		428 ± 4	
5.9–6.1	410 ± 7	(518 ± 12)	298 ± 16	396 ± 5
8.8–9.2	412 ± 7	(538 ± 15)	300 ± 17	417 ± 5
11.8–12.2	426 ± 7	(430 ± 11)	500 ± 37	397 ± 6
14.7–15.2	434 ± 7	(520 ± 14)	305 ± 19	413 ± 7
17.8–18.2	427 ± 8	(562 ± 20)	420 ± 27	387 ± 7
20.6–21.3	437 ± 9	(1120 ± 130)	408 ± 71	327 ± 8

those for the $\partial f \sim (0.14–0.27)$ transition between solution and gel cocktails, there is a definite consistency in C_f. The 19 tabulated values not affected by the cocktail transition zone (i.e. those not within parentheses in the table) have an average $C_f \simeq 397$. The changes in C_f between these values are in almost all cases within the replication uncertainties for the determination of C_f. Estimates of these uncertainties $s_m(C_f)$ can be derived from uncertainty-law propagation [ignoring $s(H,\epsilon)$ covariances for the correlations between H and ϵ] of that for the H determinations [$s_m(H)$ given above] and that for the ϵ determinations [$s_m(\epsilon)$ given below]:

$$s_m(C) \simeq C\cdot\{[s_m^2(H_1) + s_m^2(H_2)]/(H_1 - H_2)^2 + [s_m^2(\epsilon_1) + s_m^2(\epsilon_2)]/(\epsilon_1 - \epsilon_2)^2\}^{1/2}.$$

The component uncertainties $s_m(H)$ and $[s_m(\epsilon)]$, on a relative basis, are typically in the range of a few tenths of 1% (for five replicate measurements of each H and ϵ). The uncertainties in C_f, however, are largely dominated by the sometimes small $(\epsilon_1 - \epsilon_2)$ differences. As seen in Table 2, the tracking of H with ϵ is excellent for the f change $\partial f > (0.02–0.14)$ across all m regions (with an average of around $C_f \sim 420$). Considering the magnitudes of $s_m(C_f) \simeq 7$, having a 99% confidence interval of about ± 20, all of these values are essentially equivalent. A very comparable, but slightly worse result is found for the $\partial f \simeq (0.34–0.52)$ changes (with an average of around $C_f \simeq 390$ across all m). Even comparative differences between the two gel regions [$\partial f \simeq (0.27–0.34)$ and $\partial f \simeq (0.34–0.52)$ at near constant m are not too bad (on comparing columns 4 and 5 of Table 2), although a number of pairs are clearly well outside their assigned $s_m(C_f)$ uncertainties at 99% confidence. One might suppose that the tracking should have been better since the differences were all for gel-region cocktails. The substantially larger $s_m(C_f)$ uncertainties for the $\partial f \simeq (0.27–0.34)$ change may suggest that perhaps the $f \simeq 0.27$ cocktails may have been somewhat unstable because they were too close to the immiscible (neither solution nor gel) transition zone. One may reasonably conclude that the tracking of H changes with ϵ changes (or conversely the tracking of ϵ with H) for quenching by changes in f is quite good, particularly on realization that the parameter C_f used for the evaluation is very sensitive and that the evaluations were performed with very large changes in f.

The tracking between H and ϵ for quench differences imposed by changes in m, as indicated by C_m (Table 3), is decidedly less clear and more confusing. Because of the flatness of the H vs m and ϵ vs m dependencies [Figs 3(a) and 6(a)], the $(H_1 - H_2)$ and $(\epsilon_1 - \epsilon_2)$ differences comprising C_m are much smaller (compared to those for C_f). As a result, the C_m values are highly variable with estimated uncertainties $s_m(C_m)$ that can exceed the magnitude of C_m. Examination of Table 3 indicates that C_m is rarely constant (well outside their experimental uncertainties) for almost any changes in m over their broad ranges. One must conclude that ϵ (and, of necessity, the attendant quenching) is not fully tracked by changes in the quench indicating parameter H. This result will be addressed later when considering the effects of m on quench curves.

The results for C_f and C_m in Tables 3 and 4 may be expressed in a related, but somewhat more transparent form. For any ∂f or ∂m change in f or m, one can consider the percentage change in ϵ for the corresponding percentage change in H. These may be

Table 3. Tracking of the quench indicating parameter H with the LS detection efficiency ϵ for ^{3}H due to changes ∂m in total cocktail mass m at near constant H_2O mass fraction f as given by the quantity C_m. The assigned uncertainties correspond to a standard deviation of the mean $s_m(C_m)$ for 4 degrees of freedom (i.e. for the five replicate measurements of each H and ϵ used to determine C_m

f	$C_m = -(\partial H/\partial m\|_f)/(\partial\epsilon/\partial m\|_f)$					
	$\partial m \simeq (3–6)$	$\partial m \simeq (6–9)$	$\partial m \simeq (9–12)$	$\partial m \simeq (12–15)$	$\partial m \simeq (15–18)$	$\partial m \simeq (18–21)$
< 0.02	603 ± 28	253 ± 49	383 ± 103	2500 ± 2640	98 ± 46	−49 ± 25
0.14	—	537 ± 115	1330 ± 580	174 ± 41	307 ± 56	253 ± 20
0.27	211 ± 28	812 ± 270	68 ± 48	739 ± 115	147 ± 30	292 ± 17
0.34	—	203 ± 88	2330 ± 2820	273 ± 37	284 ± 17	138 ± 10
0.52	265 ± 22	2670 ± 6040	491 ± 240	269 ± 69	283 ± 49	119 ± 10

Table 4. Relative uncertainty for the measurement precision in determining the LS detection efficiency ϵ for ^{3}H, in terms of the relative standard deviation of the mean (coefficient of variation) $v_m(\epsilon)$ obtained from five replicate measurements, for 33 cocktail compositions having a total mass m and H_2O mass fraction f

Range of m (in g)	$v_m(\epsilon)$ (in %) $f < 0.02$	$f \simeq 0.14$	$f \simeq 0.27$	$f \simeq 0.34$	$f \simeq 0.52$
2.9–3.0	0.24	—	0.12	—	0.09
5.9–6.1	0.18	0.24	0.18	0.05	0.12
8.8–9.2	0.11	0.15	0.21	0.14	0.15
11.8–12.2	0.08	0.08	0.28	0.23	0.22
14.7–15.2	0.13	0.12	0.25	0.25	0.15
17.8–18.2	0.18	0.22	0.40	0.04	0.24
20.6–21.3	0.28	0.31	0.59	0.76	0.41

given by $100(\epsilon_1 - \epsilon_2)/\epsilon_1$ and $100(H_1 - H_2)/H_1$ which may be combined and expressed, for convenience, into the quantities $D_f = [(\epsilon_1 - \epsilon_2)/\epsilon_1]/[(H_1 - H_2)/H_1] = -(H_1/\epsilon_1)/C_f$ for ∂f changes and $D_m = -(H_1/\epsilon_1)/C_m$ for ∂m changes. These quantities possess the advantage of having a very simple interpretation; viz., they correspond to the percentage change in ϵ for a 1% change in H. They have the disadvantage of masking magnitudes of the differentials $\partial\epsilon/\partial H$ in the absence of knowing the values of ϵ_1 and H_1.

Figure 7 gives the observed values for D_f and D_m for adjacent (ϵ_1, H_1) and (ϵ_2, H_2) pairs within the framework of the matrix of the 33 cocktails. These results reflect the same trends discussed above for C_f and C_m.

Effects of m *and* f *on* ^3H *detection efficiency uncertainties*

Given the substantial systematic effects of m and f on the LS detection efficiencies ϵ for ^{3}H, one might naturally wonder whether m and f also influences the measurement precision in determining a particular ϵ.

Table 4 presents the results of the experimentally determined relative standard deviation of the mean (coefficient of variation) $v_m(\epsilon) = 100 \cdot s_m(\epsilon)/\epsilon$ (in %) for the various combinations of m and f. Examination of the tabulated results shows that the uncertainties $v_m(\epsilon)$ are independent of f (solution composition) for a given m, but seem to be dependent on m (cocktail size) for a given f. The wide range in $v_m(\epsilon)$ values arises from an expected broad χ^2 distribution of $s_m(\epsilon)$. Nevertheless, for every f composition, the largest $v_m(\epsilon)$ value occurs for the $m \simeq 21$ g cocktail. On averaging the $v_m(\epsilon)$ values across all f, one finds that the mean $v_m(\epsilon)$ lies within the relatively small range of 0.15–0.18% for the first four cocktail masses ($2.9 \text{ g} \leq m \leq 15.2$ g), rises to a mean value $v_m(\epsilon) \simeq 0.24\%$ for $m \simeq 18$ g, and nearly doubles again to mean $v_m(\epsilon) \simeq 0.41\%$ for $m \simeq 21$ g (see Fig. 8). In contrast, the mean $v_m(\epsilon)$ on averaging across all m lies within 0.17–0.26% for every f composition. A more complete supporting graphical analysis of the $v_m(\epsilon)$ data, similar to the one used to examine the measurement precision in H (Fig. 5), will

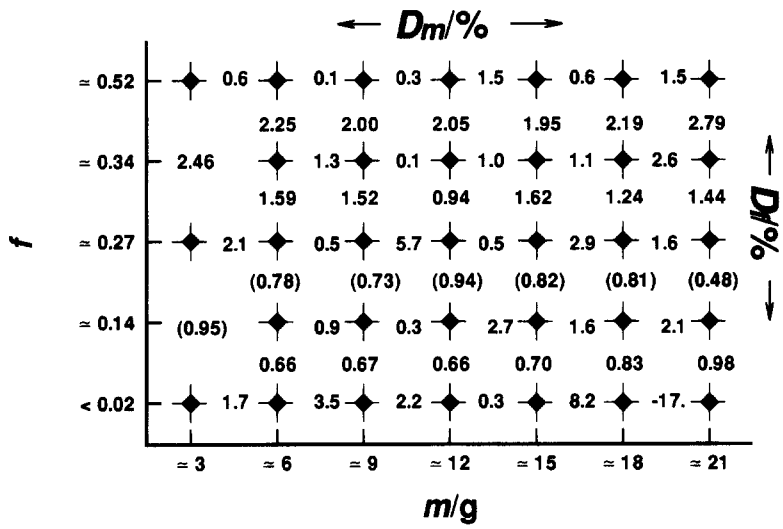

Fig. 7. Schematic tabulation of the relative tracking of the LS detection efficiency ϵ for ^{3}H with the quench indicating parameter H, as given by the quantities D_f and D_m, for the 33 cocktails. Values on the vertical lines are for D_f quench changes which result from changes ∂f in cocktail H_2O mass fraction f at near constant cocktail mass m. Those in parentheses represent D_f values for ∂f changes that correspond to transitions from solution to gel cocktails. Values on the horizontal lines are for D_m quench changes due to ∂m differences in total cocktail mass m at near constant f. Both D_f and D_m correspond to the percentage change in ϵ for a 1% change in H.

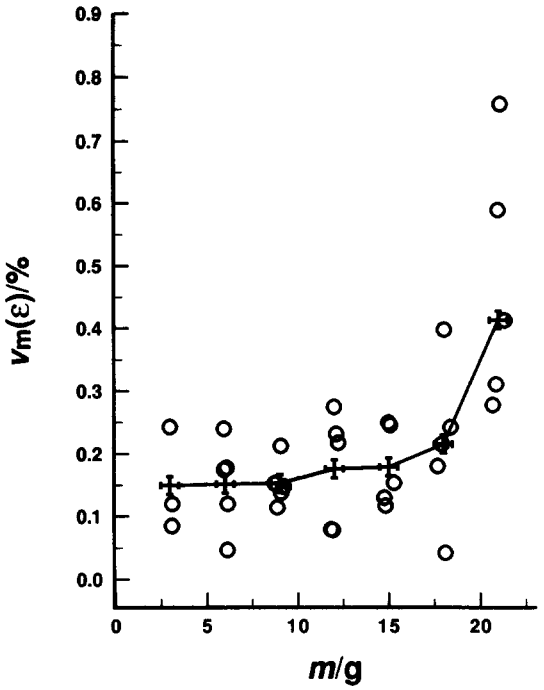

Fig. 8. Uncertainties for the determination of the LS detection efficiency ϵ for ^{3}H, in terms of the coefficient of variation $v_m(\epsilon)$ (in %), as a function of the total cocktail mass m (in g) for the five series of cocktail compositions having H_2O mass fraction f. The crosses (+) correspond to mean $v_m(\epsilon)$ values obtained from averaging across the f compositions at each m.

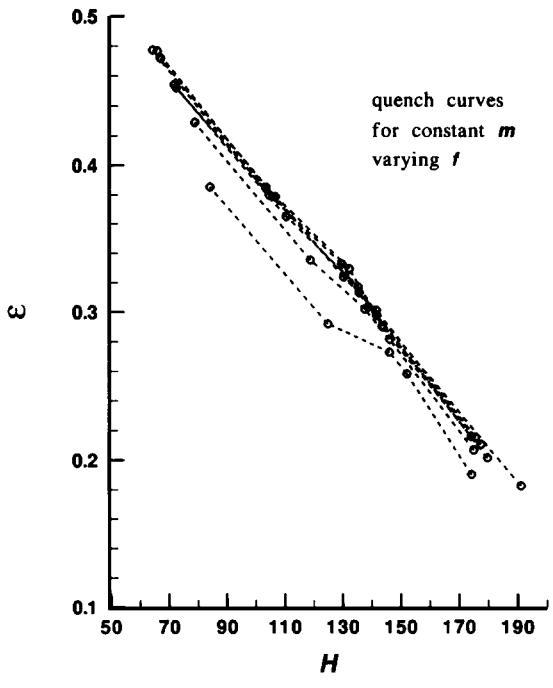

Fig. 10. The family of quench curves for the variation in LS detection efficiency ϵ for ^{3}H as a function of the quench indicating parameter H for cocktails of nearly constant total cocktail mass m and varying H_2O mass fraction f.

confirm that $v_m(\epsilon)$ is dependent on m, but is largely independent of f.

Zimmerman and Collé (1997) observed a similar kind of m-dependent effect on the reproducibility of ^{3}H-standard efficiency tracing of ^{63}Ni and ^{36}Cl. Their observation can also be ascribed to inherent differences in the efficiency measurement precision with varying cocktail sizes. They found that the reproducibilty in the efficiency-traced massic activities was distinctly poorer with both small ($m < 10$ g) and large ($m > 15$ g) cocktails, and that the magnitude of the effect was spectrometer dependent and more pronounced for the lower-energy ^{63}Ni β emitter.

Quench curves for ^{3}H with quench variations by m *and* f

Inasmuch as both m and f appear to act as types of quenching agents that influence both the QIP and detection efficiency ϵ, it is of interest to examine how these m and f variables affect a resulting ϵ vs QIP 'quench curve'.

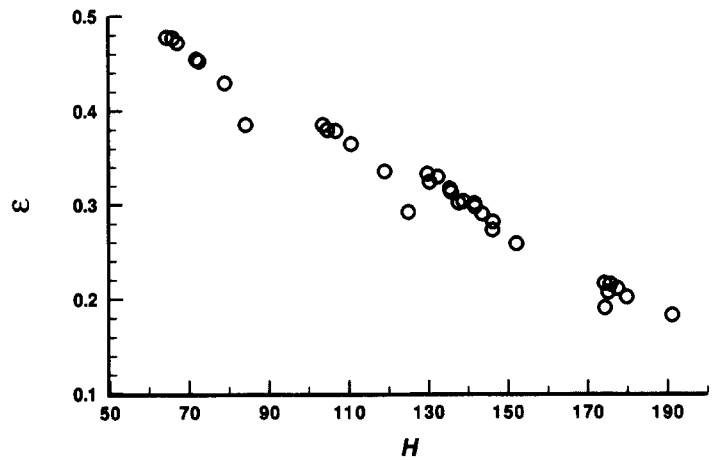

Fig. 9. An aggregate 'quench curve' for the variation in LS detection efficiency ϵ for ^{3}H as a function of the quench indicating parameter H as obtained with all 33 cocktail combinations of total cocktail mass $3 \text{ g} \leq m \leq 21$ g and H_2O mass fraction $0.002 \leq f \leq 0.52$.

To no surprise, a plot of ϵ vs H for all 33 cocktail compositions of m and f is a poor, irregularly varying representation of a quench curve (Fig. 9). It has gross discontinuities and is not a monotonic function. Rather, the aggregated data appears to consist of several superimposed and overlapping quench curves, each of which may be individually defined in terms of those having quench variations imposed by changes in m (at constant f) and those having quench variations imposed by changes in f (at constant m).

Any thought that the relationship between the detection efficiencies for some radionuclide in a series of cocktails and the determined QIP for those cocktails, irrespective of the cocktail size and composition, can be given by a single quench curve is obviously a very empty concept. The use of 'standardized quench curves' is certainly useful, and may indeed be adequate for some routine measurements having less rigorous accuracy requirements. Its adequacy in any application, however, may be dependent upon the specific systematic behavior of the cocktail series. The effect of cocktail composition is particularly paramount. The ^{36}Cl LS data of Collé and Thomas (1993) because of widely varying NaCl loadings in the cocktails, for example, exhibit cases of cocktails having nearly equal QIP values, but considerably different efficiencies; as well as the converse condition of nearly equal efficiencies, but different QIP values. This results from having multiple families of quench curves for varying aqueous fractions and varying salt content (even at near constant cocktail volume).

Figure 10 displays the family of quench curves for the seven series of cocktails with varying f and nearly constant m. The systematics are fairly regular. By now, this is to be expected since it was previously demonstrated that changes in ϵ tracked very well with changes in H when the quench differences were imposed by changes in f. In each case (i.e. for cocktails with nearly constant m), ϵ decreases

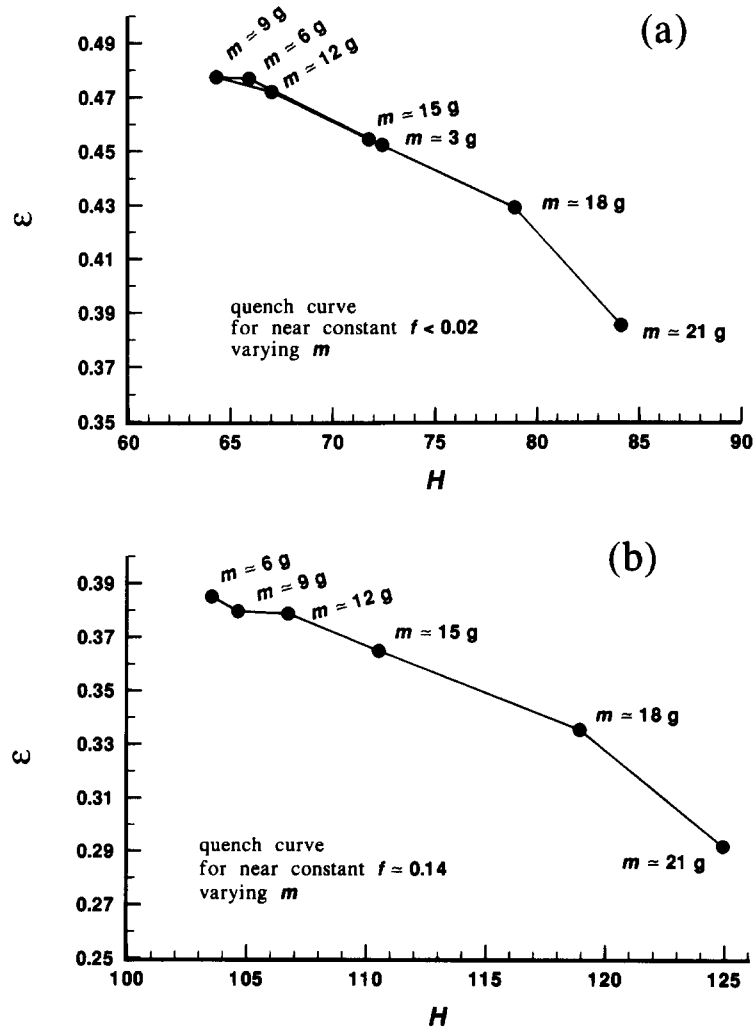

Fig. 11. Quench curves for the variation in LS detection efficiency ϵ for ^{3}H as a function of the quench indicating parameter H for *solution* cocktails of nearly constant H_2O mass fraction f and varying total mass m. The upper (a) and lower (b) curves are for the near constant $0.002 \leq f \leq 0.02$ and $f \simeq 0.14$ fractions, respectively, over the varying mass range $3\ g \leq m \leq 21\ g$.

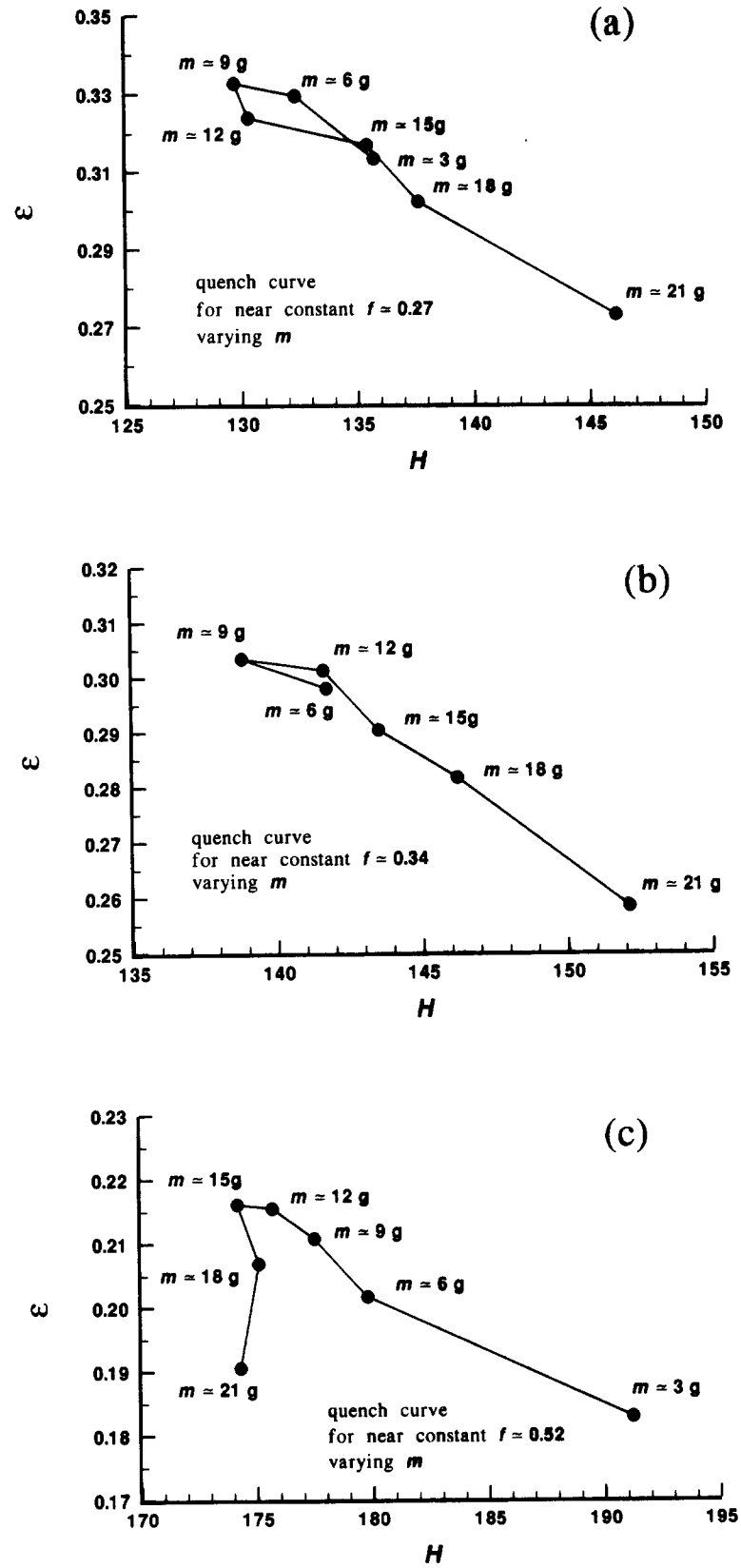

Fig. 12. Quench curves for the variation in LS detection efficiency ϵ for ^3H as a function of the quench indicating parameter H for *gel* cocktails of near constant H_20 mass fraction f and varying total mass m. The three are for $f \simeq 0.27$ [curve (a)], $f \simeq 0.34$ [curve (b)], and $f \simeq 0.52$ [curve (c)] over the varying mass range $3\ g \leq m \leq 21\ g$.

monotonically with increasing H as f increases. Each function is nominally linear (with the largest deviation from nonlinearity for the $m \simeq 21$ g curve) even though the curves are composed of data obtained with two distinct types of cocktails (gels for the lower three H values and solutions for the upper two). The locations of these individual superimposed curves with respect to each other (as determined by m), however, is exceedingly complex as will be demonstrated.

The quench curves for the two solution cocktails as generated by varying m are shown in Fig. 11. For the cocktail series with $f \simeq 0.14$ [Fig. 11(b)], there is a fairly systematic and regular monotonic decrease in ϵ with increasing H as m increases. The other, for $0.002 \leq f \leq 0.02$, shows a somewhat similar pattern, *excepting* that the $m \simeq 3$ and 6 g values get 'folded back' onto the lower portions of the quench curve [Fig. 11(a)]. This same effect was not explicitly noted, but can also be found in the quench curve data of Zimmerman and Collé (1997) for their volume variations with nearly constant $f \simeq 0.05$ cocktails. Their results for the variation in ϵ with H shows a 'folding back' of an $m \simeq 5.3$ g datum onto their fairly linear quench curve such that it lies between the points for $m \simeq 10.3$ and 12.7 g. The quench curve obtained by them for the same cocktail series with a second spectrometer (that employed a different external-source, Compton-spectrum-based QIP) exhibited a 'folding back' of two values: an $m \simeq 7.7$ g to just below that for $m \simeq 10.3$ g, and the $m \simeq 5.3$ g point to between those for $m \simeq 12.7$ and 15.2 g.

This irregular m-varying quench curve behavior becomes even more bizarre for the gel cocktails (Fig. 12). With increasing f, more points of the quench curve appear to get 'folded back', and the curve begins to separate into two distinct portions. The systematics across the gamut of these m-varying quench curves, based on a sequential perusal, is striking. If one starts with the $f \simeq 0.14$ solution cocktails [Fig. 11(b)], one observes considerable regularity with a systematic, near-linear, monotonic decrease in ϵ with increasing H as m increases. For the other $0.002 \leq f \leq 0.02$ (minimally quenched) solution cocktails [Fig. 11(a)], one finds that the quench curve points for the cocktails of lowest mass ($m \simeq 3$ and 6 g) are 'folded back' into the curve. The ϵ vs H functionality is still fairly regular with a monotonic decrease in ϵ with increasing H, although the point for the $m \simeq 21$ g cocktail departs substantially from linearity. Moving to the opposite extreme of the curves for the more quenched gel cocktails, one finds quench curves for the $f \simeq 0.27$ [Fig. 12(a)] and $f \simeq 0.34$ [Fig. 12(b)] cocktails that are roughly similar to that found for the $0.002 \leq f \leq 0.02$ cocktails. The dispersion in the points on the curves for the 'folded back' portions, however, are somewhat greater. By the time one reaches the $f \simeq 0.52$ quench curve [Fig. 12(c)], the relation between ϵ and H is almost uncorrelated so much so that the line defining the $m \simeq 15$, 18 and 21 g points is nearly vertical and at an acute angle to the remaining portion of the m-varying quench curve.

If nothing else, the above systematic analysis clearly demonstrates that cocktail size (m) variation is an exceedingly poor imposed quenching agent. Quenching imposed by variations in cocktail composition, such as the linear parameter f used here, is clearly better, and how well it does depends largely on the range of composition changes. It may not be much better over very broad unsystematic composition changes, such as when cocktails contain differing constituents in the radioactive solution aliquants (mineral acids, dissolved salts, etc.).

Summary Findings and Concluding Implications

This systematic evaluation of the total cocktail mass m and H_2O mass fraction f on the $4\pi\beta$ LS spectrometry of ^3H revealed some obvious and some newly-discerned, not-so-obvious findings. Among them are:

1. The background counting rate of a LS cocktail increases, as expected, with the increasing geometrical efficiency of cocktails with larger m and with the decreasing quenching of cocktails with smaller f.

2. Careful evaluations of the background uncertainty can elucidate the relative magnitudes of this uncertainty's components.

3. Compton-edge-based quench indicating parameters (QIP), a Horrocks number H, are not only strongly influenced by f-varying chemical quench changes (as expected), but are also dependent on m.

4. At least some part of the complex m dependence on H must be due to some external effect beyond any internal quenching in the cocktail (probably the subtended solid angles for the geometrical arrangement amongst the external γ-ray source used for the quench monitoring, the cocktail volume in the LS vial, and the photomultiplier tubes).

5. The uncertainty (measurement replication precision) in making an H determination appears to be independent of m and f, as well as the magnitude of H itself, which suggests that this uncertainty is largely of fixed magnitude (for a given LS system) and controlled by the precision in locating the channel-number position of the Compton edge irrespective of the magnitude of the Compton-edge shift with quenching.

6. The LS detection efficiency for ^3H has an obvious monotonic functionality with the increased quenching associated with increasing f, and has a complex dependence on m that somewhat parallels (inversely) the H vs m dependence.

7. The uncertainties (replication precision) in determining ϵ were slightly dependent on m (cocktail size) at near constant f, but were largely invariant of f (cocktail composition) at near constant m.

8. The 'optimum' (i.e. maximum efficiency) $m \simeq 9$ g cocktail size for *solution* cocktails agreed

with a canonically accepted value of 8–12 mL, but for *gel* cocktails the maximum efficiency shifted to larger m values as f increased.

9. The dependence of both H and ϵ with changes in m tended to 'flatten' with increasing f (i.e. $\partial\epsilon/\partial m|_f$ and $\partial H/\partial m|_f$ were much less at large f values than at small ones).

10. The ^{3}H efficiency dependencies on m and f are not fully tracked by the inverse H dependencies on m and f.

11. Observed discrepancies in the ϵ vs H quench curves for variable m (at near constant f) exhibit a peculiar 'folding over' of the quench curve.

12. Quench variations induced simultaneously by multiple factors (e.g. m and f) exhibit a very complex ϵ vs H behavior that is largely a result of having multiple families of superimposed quench curves.

These findings have several significant implications. The most obvious is that efficiency changes cannot be adequately monitored by quench indicating parameters when the quench changes are induced by multiple causal factors (e.g. simultaneously varying cocktail sizes and compositions). This implication can, in turn, result in repercussive inherent errors in radionuclidic assays which are performed by LS spectrometry. The errors result from cocktail mismatching effects that cannot be fully accounted for by quench monitoring compensations. Such cocktail-mismatch errors can occur not only in comparative ^{3}H measurements using developed quench curves, but also in the more exacting ^{3}H-standard efficiency tracing methods. These implications and supporting analyses are treated at length in a companion paper (Collé, 1997).

Acknowledgements—The author heartily thanks and acknowledges Dr Raj Kishore (Food and Drug Administration, U.S. Department of Health and Human Services), a guest worker in the Radioactivity Group of the NIST Physics Laboratory (Ionizing Radiation Division) during 1989–1990, for laboratory assistance with some of the initial aspects of the sample preparations; Mme Dr K. A. Maroufi-Collé for highly-valued organizational efforts in uncovering the 'rediscovered' LS data; and his esteemed colleagues, Drs B. E. Zimmerman and B. M. Coursey, for their insightful reflections and discussions on LS spectrometry effects. The National Institute of Standards and Technology (NIST) is an agency of the Technology Administration of the U.S. Department of Commerce. Certain commercial equipment, instruments, or materials are identified in this paper to foster understanding. Such identification does not imply recommendation or endorsement by NIST, nor does it imply that the materials or equipment identified are necessarily the best available for the purpose.

References

Amersham Corp. (September, 1981) PCS: A complete Phase Combining System for scintillation counting of radioactive aqueous solutions, data sheet. Amersham Corp., Arlington Heights, Ill.

Collé R. and Thomas J. W. L. (1993) ^{36}Cl/Cl accelerator-mass-spectrometry standards: verification of their serial-dilution-solution preparations by radioactivity standards. *J. Res. Natl. Inst. Stds. Tech.* **98,** 653–677.

Collé R. A. (1995) Precise determination of the ^{222}Rn half-life by 4π-$\alpha\beta$ liquid scintillation measurements. *Radioact. Radiochem.* **6,** 16–29.

Collé, R. (1997) Cocktail mismatch effects in $4\pi\beta$ liquid scintillation spectrometry: implications based on the systematics of ^{3}H detection efficiency and quench indicating parameter variations with total cocktail mass (volume) and H_2O fraction. *Appl. Radiat. Isot.* **48,** 833–842.

Collé, R. and Zimmerman, B. E. (1996a) ^{63}Ni half-life: a new experimental determination and critical review. *Appl. Radiat. Isot.* **47,** 677–691.

Collé, R. and Zimmerman, B. E. (1996b) ^{63}Ni standardization: 1968–1995 **7**(2), 12–27.

National Institute of Standards and Technology (NIST) (January, 1989) Certificate, Radioactivity Standard, Hydrogen-3, Standard Reference Material SRM 4927D. NIST, Gaithersburg, MD.

Zimmerman, B. E. and Collé, R. (1997) Cocktail volume effects in $4\pi\beta$ liquid scintillation spectrometry with ^{3}H-standard efficiency tracing for low-energy β-emitting radionuclides. *Appl. Radiat. Isot.* **48,** 365–378.